Bioorganic & Medicinal Chemistry 19 (2011) 7023–7032

Contents lists available at SciVerse ScienceDirect

Bioorganic & Medicinal Chemistry

journal homepage: www.elsevier.com/locate/bmc

Design, synthesis, and biological evaluation of a novel series of bisintercalating DNA-binding piperazine-linked bisanthrapyrazole compounds as anticancer agents

Rui Zhang [a], Xing Wu [a], Jack C. Yalowich [b], Brian B. Hasinoff [a,*]

[a] Faculty of Pharmacy, Apotex Centre, University of Manitoba, 750 McDermot Avenue, Winnipeg, Manitoba, Canada R3E 0T5
[b] College of Pharmacy, The Ohio State University, 500 West 12th Avenue, Columbus, OH 43210, USA

ARTICLE INFO

Article history:
Received 27 July 2011
Revised 23 September 2011
Accepted 5 October 2011
Available online 14 October 2011

Keywords:
Bisanthrapyrazole
Bisintercalating
Anticancer
DNA
DNA-binding
Topoisomerase
Molecular modeling
Docking
K562 cells
Cardiotoxic

ABSTRACT

A series of bisintercalating DNA binding bisanthrapyrazole compounds containing piperazine linkers were designed by molecular modeling and docking techniques. Because the anthrapyrazoles are not quinones they are unable to be reductively activated like doxorubicin and other anthracyclines and thus they should not be cardiotoxic. The concentration dependent increase in DNA melting temperature was used to determine the strength of DNA binding and the bisintercalation potential of the compounds. Compounds with more than a three-carbon linker that could span four DNA base pairs achieved bisintercalation. All of the bisanthrapyrazoles inhibited human erythroleukemic K562 cell growth in the low to submicromolar concentration range. They also strongly inhibited the decatenation activity of topoisomerase IIα and the relaxation activity of topoisomerase I. However, as measured by their ability to induce double strand breaks in plasmid DNA, the bisanthrapyrazole compounds did not act as topoisomerase IIα poisons. In conclusion, a novel group of bisanthrapyrazole compounds were designed, synthesized, and biologically evaluated as potential anticancer agents.

1. Introduction

DNA binding anticancer drugs such as doxorubicin and the other anthracyclines, amsacrine, and mitoxantrone are some of the most widely used and efficacious anticancer drugs. Typically these DNA intercalating drugs inhibit DNA topoisomerase II and induce DNA double strand breaks and cell death.[1,2] Drugs that intercalate into DNA might also be expected to inhibit cell growth through interference with topoisomerase I and other DNA processing enzymes. Doxorubicin and the other anthracyclines are quinones and can be reductively activated to produce damaging reactive oxygen species that may lead to a potentially fatal cardiotoxicity. However, the anthrapyrazoles, while structurally similar to the anthracyclines, do not contain a quinone moiety and cannot be reductively activated, and thus they should not be cardiotoxic. In previous studies, using molecular modeling and docking techniques, we designed monointercalating[3] and bisintercalating[4,5] anthrapyrazole analogs of losoxantrone and piroxantrone that exhibited potent cancer cell growth inhibitory effects. More recently, we reported the synthesis and biological evaluation of monointercalating anthrapyrazole combilexins with DNA minor groove binding netropsin-like oligopyrrole carboxamide side chains.[6] In principle, bisintercalating molecules should be able to interact more strongly with DNA and thus should have a prolonged residence time on DNA allowing them to interfere with DNA processing enzymes.[7–10] Bisintercalators should also, in principle, have enhanced DNA sequence specificity compared to monointercalators or minor groove binders. However, because intercalators typically only have a slight preference for GC base-pairs, sequence specificity may not necessarily be achieved. Bisintercalating compounds, as exemplified by echinomycin, occur naturally and it and several purely synthetic compounds have progressed into clinical trials as antitumor agents.[7,9–12]

In this study, we have designed, synthesized, and biologically evaluated a series of mono- and bisanthrapyrazole compounds containing piperazine linkers (Fig. 1) based on the DNA intercalating anthrapyrazoles. Piperazine-containing linkers have been previously used with bisintercalating imidazoacridone,[13] phthalazine,[14] and quinoline, cinnoline and phthalimide moieties.[15] The bisanthrapyrazoles were designed with tertiary amines in the linkers so that they would be positively charged at physiological pH in order to

* Corresponding author. Tel.: +1 204 474 8325; fax: +1 204 474 7617.
E-mail address: B_Hasinoff@UManitoba.ca (B.B. Hasinoff).

0968-0896/$ - see front matter © 2011 Elsevier Ltd. All rights reserved.
doi:10.1016/j.bmc.2011.10.012

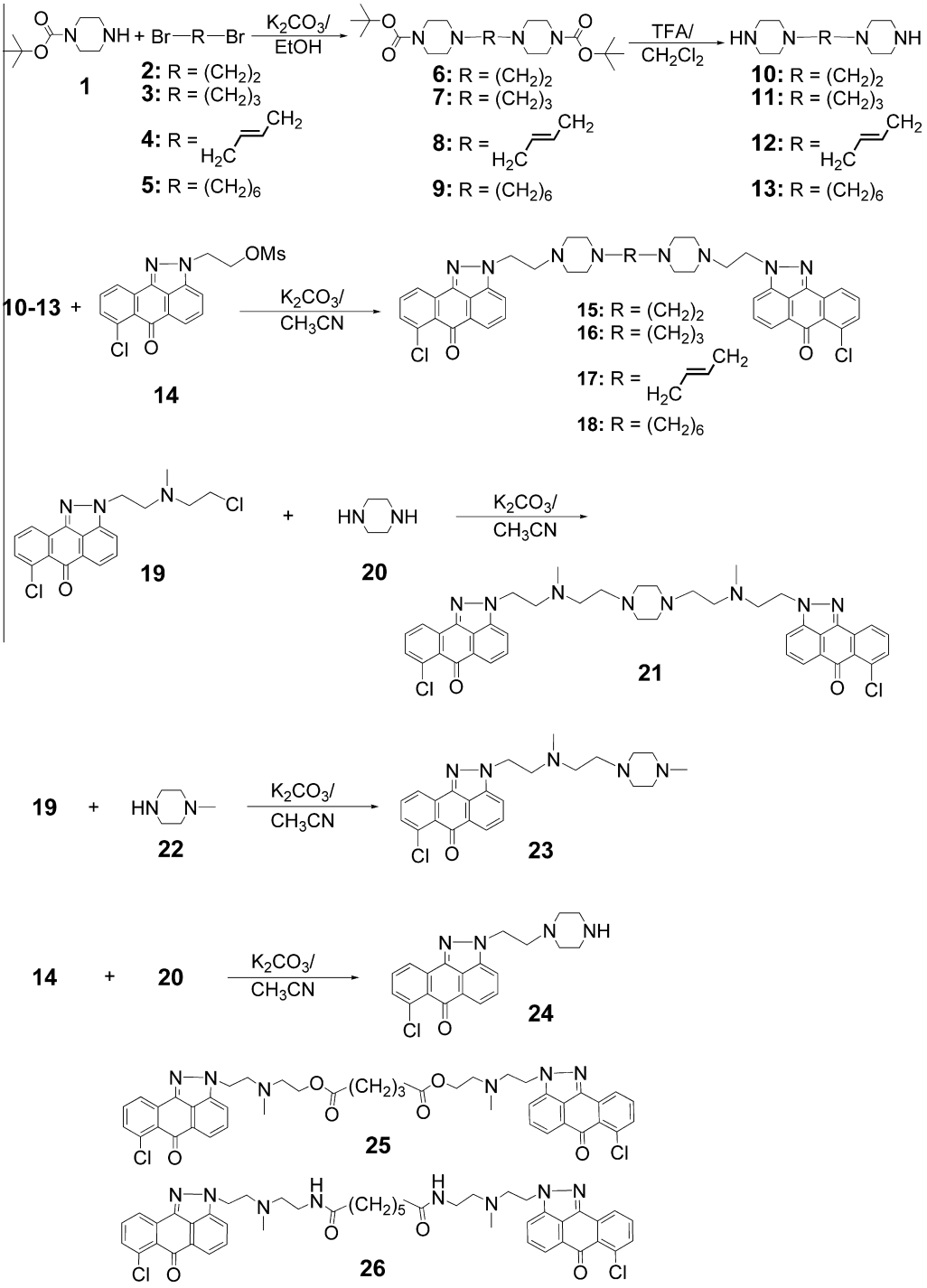

Figure 1. Reaction scheme and structures for the synthesis of the piperazine-linked bisanthrapyrazoles compounds **15**–**18** and **21**, their monointercalating analogs **23** and **24** and their precursors. Compounds **25** and **26** are the most potent ester-linked[4] and amide-linked[5] bisanthrapyrazoles that were previously synthesized.

favor electrostatic interactions in the minor groove with the anionic phosphate DNA backbone. Also because some tumor cells preferentially take up polyamines via the polyamine transport system,[16,17] a polyamine piperazine linker would be expected to facilitate uptake of the piperazine-linked bisanthrapyrazoles. The polyamine-linked etoposide analog F14512 that targets topoisomerase II has been specifically designed to exploit this transport system.[17] In addition to measuring the cell growth inhibitory effects of these compounds, we also measured their ability to bind to DNA, to inhibit topoisomerase I, topoisomerase IIα, and to induce topoisomerase IIα-mediated DNA cleavage.

2. Results

2.1. Synthesis of the mono- and bisanthrapyrazole piperazines

The piperazine-linked bisanthrapyrazoles **15**–**18**, **21**, and piperazine-modified anthrapyrazoles **23**, **24** were synthesized as shown in Figure 1. The bispiperazine intermediates **10**–**13** were prepared in 70–90% yields via reaction of commercially available *t*-Boc protected piperazine **1** with the dibromoalkanes **2**, **3**, **5**, and (*E*)-1,4-dibromobut-2-ene **4** followed by deprotection of the *t*-Boc group under acidic conditions as described.[18] The bispiperazines **10**–**13**

were then reacted with mesylated anthrapyrazole **14** in the presence of K_2CO_3 to afford bisanthrapyrazoles **15**–**18** in 40–45% yields. Using the same method the reaction of piperazine with anthrapyrazole **19** yielded the bisanthrapyrazole **21** in 30% yield. Anthrapyrazole **23**, with a methylpiperazine side chain was afforded in 57% yield by the reaction of **19** with 1-methylpiperazine. Mesylated anthrapyrazole **14** reacted with excess piperazine to afford the monoanthrapyrazole **24** in 50% yield.

2.2. Effect of the mono- and bisanthrapyrazole piperazines on the thermal denaturation of DNA

The increase in DNA melting temperature ΔT_m with increasing concentration of the newly synthesized compounds is shown in Figure 2A and B. Table 1 reports the ΔT_m of sonicated calf thymus DNA induced by 1 μM of the mono- and bisanthrapyrazole piperazine compounds. Three of the compounds, **17**, **18**, and **21**, increased T_m more than the positive control, the strong DNA intercalator doxorubicin, which increased T_m by 8.4 °C. Compounds **17**, **18**, and **21** are all bisanthrapyrazoles that have longer linkers. The compound that increased T_m the most (ΔT_m of 14.9 °C) was the bisanthrapyrazole **21** which contained a single piperazine and two methyl amino groups in the linker. These tertiary amines would be partially protonated at biological pH, which should result in an enhanced electrostatic interaction with anionic DNA. Compounds **23** and **24**, which are monoanthrapyrazoles with a piperazine-containing side chain, had ΔT_m values of 5.1 and 5.3 °C, respectively, indicating that they bound to DNA more weakly than their respective bisanthrapyrazole congeners, **21** and **17**–**18**.

In our previous studies on the analogous ester- and amide-linked bisanthrapyrazoles[4,5] we showed that the slope of drug concentration versus ΔT_m plot for a bisintercalator is approximately twice that of its corresponding monomeric monointercalator. This has also been shown from a comparison of the ΔT_m values of the bisintercalator dye YOYO and its monomeric form YO-PRO.[19] This is due to the bisintercalator occupying twice the number of intercalation sites on the DNA and is based on a simple model in which the different intercalation sites contribute equally and independently to the free energy difference between the hybridized and melted states. In this model, the presence of an intercalator at a site lowers the free energy of the hybridized state by a fixed, site-independent amount.[19] Thus, the increase in the melting temperature of a DNA duplex should increase in proportion to the number of intercalated groups. Given the assumptions this is, of course, a highly simplified model. Under the limiting conditions used, the value of ΔT_m is directly proportional to the logarithm of the equilibrium constant and hence the free energy.[20] The concentration dependence of ΔT_m for monomeric **24** and the bisanthrapyrazoles **15**, **16**, **17**, and **18** are shown in Figure 2A. A *t*-test comparison of the slopes showed that compounds **17** and **18** had slopes that were significantly different ($p = 0.0008$ and 0.005, respectively) than monomer **24**. The slopes of the plots of **17** and **18** were 1.8 ± 0.3 and 1.8 ± 0.3-fold (mean ± SEM) larger, respectively, than that for the monoanthrapyrazole **24** which suggests that **17** and **18** achieved good bisintercalation. The SEMs were calculated from a propagation of errors analysis. Compound **16** with a three-methylene linker had a slope that was 1.4 ± 0.2-fold larger and only just significantly different ($p = 0.03$) than that of **24** which suggests that **16** formed a mixture of mono- and bisintercalating complexes. Together these results suggest that compounds with a bispiperazine linker needed at least a four-carbon linker to achieve bisintercalation. The concentration dependence of ΔT_m for monomeric **23** and the bisanthrapyrazole **21** are shown in Figure 2B. The slope for **21** was 2.9 ± 0.1-fold larger than for **23**, a result which suggests that **21** achieved bisintercalation as well. Compound **15** with a two-carbon linker had a slope that was significantly less ($p = 0.005$) than the monomer **24**. This result suggests that **15** may not have achieved bisintercalation into DNA.

2.3. Effect of the mono- and bisanthrapyrazole piperazines on the inhibition of the decatenation activity of topoisomerase IIα, on the stabilization of the covalent topoisomerase IIα-DNA cleavable complex, and the inhibition of the relaxation activity of topoisomerase I

The torsional stress that occurs in DNA during replication and transcription and daughter strand separation during mitosis can be relieved by topoisomerase II. Topoisomerase II alters DNA topology by catalyzing the passing of an intact DNA double helix through a transient double-stranded break made in a second helix.[21,22] The ability of 20 μM of the compounds to inhibit the decatenation of concatenated kDNA by topoisomerase IIα was determined as previously described.[6,23] Densitometry of the fully decatenated open circular DNA bands in the gel image of Figure 3A was used to calculate the percentage inhibition data of Table 1. As shown in Table 1 all of the compounds, including the monoanthrapyrazoles, strongly

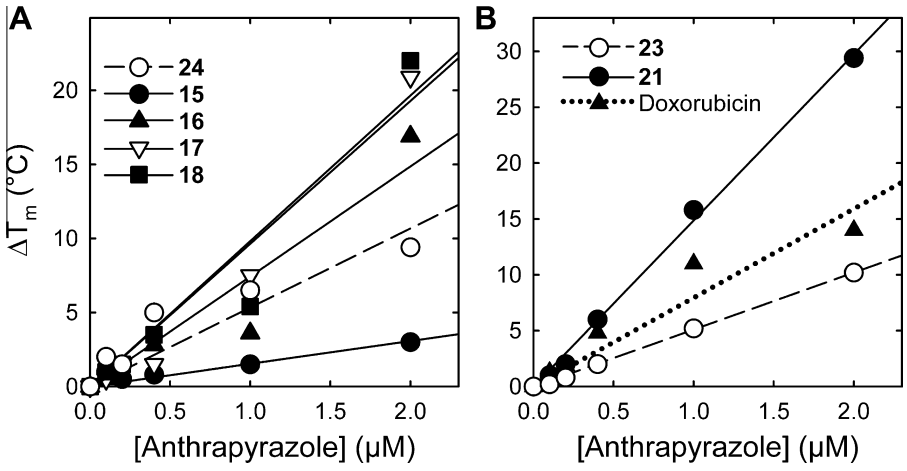

Figure 2. Concentration dependence of ΔT_m for the mono- and bisanthrapyrazoles binding to DNA. (A) Concentration dependence of ΔT_m for the monoanthrapyrazole **24** and the bisanthrapyrazoles **15**–**18**. Compounds with slopes approximately twice that of the parent monomer **24** indicate that they formed bisintercalation complexes with DNA. (B) Concentration dependence of ΔT_m for the monoanthrapyrazole **23**, the bisanthrapyrazole **21** and doxorubicin for comparison. The straight lines were linear least-squares calculated fits to the data.

Table 1
DNA binding, cell growth inhibition, topoisomerase IIα and topoisomerase I inhibitory effects of the mono- and bis piperazine-linked anthrapyrazoles and some previously synthesized ester- and amide-linked bisanthrapyrazoles

Compound	ΔT_m[a] (°C)	Cell growth inhibition		Resistance factor[b]	Topoisomerase IIα		Topoisomerase I
		K562 IC_{50} (μM)	K/VP.5 IC_{50} (μM)		% Inhibition[c]	% Cleavage[d]	% Inhibition[e]
15	1.5	6.6	9.3	1.4	92	2	ND
16	7.4	0.97	1.33	1.4	98	0	ND
17	9.6	0.52	0.58	1.1	100	0	ND
18	9.8	0.24	0.52	2.1	100	0	ND
21	14.9	0.50	0.71	1.4	88	5	ND
23	5.1	10.5	5.2	0.5	87	0	100
24	5.3	0.47	0.35	0.7	100	0	100
25[f]	4.2	1.1	2.9	2.6	20	0	ND
26[g]	2.4	4.6	2.5	0.6	40	0	ND
Doxorubicin[h]	8.4	0.033	0.52	15.9	30	0	ND

ND is not determined due to band shifting and smearing on the gels.
[a] Least-squares calculated best fit value at 1 μM.
[b] The resistance factor was calculated from the ratio of the IC_{50} value for the K/VP.5 cell line divided by that for the K562 cell line.
[c] At 20 μM.
[d] At 50 μM. % Cleavage values are from relative to amounts of linear DNA produced by 50 μM etoposide (100%) less the no-drug control value (approximately 2%).
[e] At 20 μM. It was not possible to evaluate the topoisomerase I inhibitory activity of compounds **15**–**21** because of band shifting and broadening due to strong binding to DNA.
[f] Derived from Ref. 4
[g] Derived from Ref. 4
[h] From Ref. 6

inhibited the decatenation activity of human topoisomerase IIα. For comparison, doxorubicin (at 20 μM) inhibited the decatenation activity of topoisomerase IIα by 30%.

The decatenation assay is a measure of the ability of these compounds to inhibit the catalytic activity only. Thus, this assay is not a measure of whether these compounds acted as topoisomerase II poisons as do some widely used anticancer drugs such as the anthracyclines, piroxantrone, losoxantrone, mitoxantrone, and etoposide.[21,22,24,25] These "so called" topoisomerase II poisons exert their cytotoxicity through their ability to stabilize a covalent topoisomerase II-DNA intermediate (the cleavable complex). Stabilization of the covalent complex leads to double strand DNA breaks that are toxic to the cell. Thus, DNA cleavage assay experiments,[26] as we previously described[3–6,27] were carried out to see whether 50 μM of the compounds stabilized the cleavable complex using etoposide as a positive control. As shown in Figure 3B the addition of etoposide (lane 10) to the reaction mixture containing topoisomerase IIα and supercoiled pBR322 DNA induced formation of linear pBR322 DNA. Linear DNA was identified by comparison with linear pBR322 DNA produced by action of the restriction enzyme *HindIII* acting on a single site on pBR322 DNA (not shown). Based on integrated band intensities of linear DNA in Figure 3B, the compounds of Table 1 induced little or no measurable formation of linear DNA. Thus, at least compared to etoposide, they did not act as topoisomerase IIα poisons through stabilization of the covalent DNA-topoisomerase II cleavage complex.

Experiments to determine if the compounds of Table 1 could inhibit the topoisomerase I relaxing activity of supercoiled pBR322 DNA were carried out as we previously described.[6,28] Topoisomerase I is a DNA processing enzyme[29] that relieves torsional stress in DNA. Unlike topoisomerase II, topoisomerase I does not require an ATP cofactor. Topoisomerase I relaxes DNA through a transient single strand break in DNA as compared to the transient double strand break in DNA induced by topoisomerase II.[29] As shown by the gel image in Figure 4, the monoanthrapyrazoles **23** and **24** (at 20 μM) strongly inhibited the relaxation activity of topoisomerase I towards supercoiled pBR322 DNA. The well known topoisomerase I inhibitor camptothecin at 20 μM was used as a positive control.[29] It was not possible to determine whether the bisanthrapyrazoles (**15**–**18** and **21**) tested were also topoisomerase I inhibitors due to band shifts and smearing on the gel. The band shifting and smearing was likely due to the strong binding of these compounds to DNA that changed their electrophoretic mobility. This assay was run in the absence of ethidium bromide in order to obtain sufficient separation between the relaxed and supercoiled DNA. After electrophoresis the gel was treated with ethidium bromide to visualize the DNA.

2.4. Cell growth inhibitory effects of the mono- and bisanthrapyrazole piperazines on human leukemia K562 cells and K/VP.5 cells with a decreased level of topoisomerase IIα

Cancer cells can acquire resistance to topoisomerase II poisons by lowering their level and/or activity of topoisomerase II.[21,30] We previously used[3–6] a clonal K562 cell line selected for resistance to etoposide as a screen to determine the ability of compounds to act as topoisomerase II poisons. The etoposide-selected K/VP.5 cells are 26-fold resistant to etoposide and contain reduced levels of both topoisomerase IIα (six-fold) and topoisomerase IIß (three-fold).[31,32] In addition, these cells are cross resistant to other known topoisomerase II poisons.[33] If there is less topoisomerase II in the cell, fewer DNA strand breaks are produced by topoisomerase II poisons which results in reduced cytotoxicity.

As shown in Table 1 all of the mono- and bisanthrapyrazole piperazines potently inhibited the growth of K562 and K/VP.5 cells in the low- to submicromolar range as measured by their IC_{50} values. Compound **18**, which contains a six-carbon linker, was the most potent. The bisanthrapyrazoles **17** and **21** with longer linkers also achieved submicromolar IC_{50} values.

Most of the compounds in Table 1 displayed little or no cross resistance to K/VP.5 cells. In contrast, K/VP.5 cells were found to be 15.9-fold resistant to the intercalating topoisomerase II poison, doxorubicin.[6] Thus, both these results and the results of the cleavage assay (Table 1, Fig. 3B) indicate that none of these compounds inhibited cell growth by acting as topoisomerase II poisons.

2.5. Docking of the mono- and bisanthrapyrazole piperazines into DNA

In order to determine possible DNA binding conformations, the mono- and bisanthrapyrazole piperazines were docked into an X-ray structure of DNA (Fig. 5). The X-ray structure used (PDB ID:

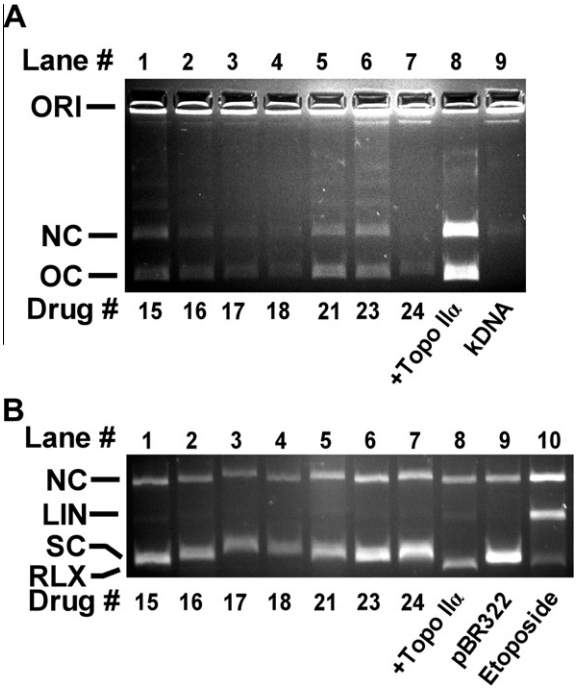

Figure 3. Effect of the mono- and bisanthrapyrazoles on the catalytic decatenation activity and the cleavable complex forming ability of topoisomerase IIα. (A) Effect of mono- and bisanthrapyrazoles on the topoisomerase IIα-mediated decatenation activity of kDNA. This fluorescent image of the ethidium bromide containing gel shows that topoisomerase IIα (Topo IIα) decatenated kDNA to its open circular (OC) form (lane 8). Topoisomerase IIα was present in the reaction mixture for all lanes but lane 9. ORI is the gel origin. All drugs, except where indicated, were present at a concentration of 20 μM in the assay mixture. All of the compounds strongly inhibited the decatenation activity of topoisomerase IIα. (B) Effect of the mono- and bisanthrapyrazoles and etoposide on the topoisomerase IIα-mediated relaxation and cleavage of supercoiled pBR322 plasmid DNA. This fluorescent image of the ethidium bromide-stained gel shows that topoisomerase IIα (Topo IIα) converted supercoiled (SC) pBR322 DNA (lane 9) to relaxed (RLX) DNA (lane 8). In this assay the relaxed DNA runs slightly ahead of the supercoiled DNA because the gel was run in the presence of ethidium bromide. Topoisomerase IIα was present in the reaction mixture in all but lane 9. As shown in lane 10, etoposide treatment produced significant amounts of linear DNA (LIN). A small amount of nicked circular (NC) is normally present in the pBR322 DNA. A densitometric analysis of the linear DNA bands showed that all the compounds produced much less linear DNA than the etoposide positive control (lane 10). The concentration of all test compounds in the cleavage assay mixture was 50 μM. Even though the gel was run in the presence of ethidium bromide some of the compounds (e.g., **16** and **17**) caused a band shift likely due to strong binding to DNA.

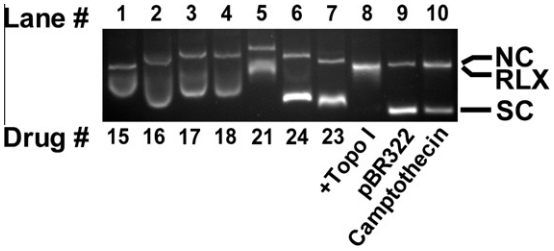

Figure 4. Effect of the mono- and bisanthrapyrazoles and camptothecin on the ability of topoisomerase I to relax supercoiled pBR322 DNA. This fluorescent image of the ethidium bromide-stained gel shows that most of the compounds detectably inhibited the relaxation activity of topoisomerase I. The topoisomerase I inhibitor camptothecin was used as a positive control. All lanes except lane 9 contained topoisomerase I. All drugs, except where indicated, were present at a concentration of 20 μM in the assay mixture. In this gel, which was stained with ethidium bromide after it was run, the supercoiled DNA (SC) ran ahead of the relaxed DNA (RLX). The relaxed DNA was not well resolved from the nicked circular DNA (NC). Based on densitometric analysis of the supercoiled band camptothecin inhibited the relaxation activity by about 50% while the monoanthrapyrazole **23** and **24** caused approximately 100% inhibition. Because the gel was not run in the presence of ethidium bromide, most of the bisanthrapyrazole compounds induced significant band shifts, likely due to strong binding to DNA. Hence, it was not possible to reliably quantitate the degree of inhibition of some of the bisanthrapyrazole compounds.

1DA9)[34] is a complex with two molecules of doxorubicin separated by four base pairs intercalated into duplex DNA. In this structure, the planar doxorubicin molecule induces outward bulges in the base pairs directly above and below it. The docking of **18** into the 1DA9 structure (Fig. 5A) showed that both anthrapyrazoles docked with their aromatic rings coplanar with the DNA bases in a configuration similar to doxorubicin. However, compound **15** with the shortest linker (two methylene groups) did not achieve bisintercalation (Fig. 5B). While one anthrapyrazole moiety of **15** was well intercalated, the other anthrapyrazole moiety was positioned mainly in the minor groove. While compound **17** with a four-carbon linker also achieved a good bisintercalation pose, compound **21** displayed a pose in which one of the anthrapyrazole groups was largely, but still only partially, intercalated into the second binding site (Fig. 5C). Likewise, compound **16** was only partially, intercalated into the second binding site (structure not shown). Compound **15** was also docked into an X-ray structure of a netropsin-DNA complex (PDB ID: 195D)[35] in order to see if this compound, which did not dock as a bisintercalator, could bind to DNA in the minor groove. Netropsin is a well known minor groove binder.[35] Compound **15** docked into the minor groove and had good overlap with the netropsin in the minor groove (structure not shown). Thus **15** may have functioned both as a minor groove binder and a monointercalator.

2.6. QSAR correlation analyses of DNA binding affinity and K562 cell growth inhibition

A correlation analysis was carried out on the ΔT_m values versus the K562 $\log IC_{50}$ values for the mono- and bisanthrapyrazoles **15**, **16**, **17**, **18**, and **24** of Table 1. The ΔT_m values were correlated with the K562 $\log IC_{50}$ values with a r^2 of 0.74 and a p value for the slope that was close to statistically significant (p of 0.06). The slope of a separate plot for compounds **23** and **21**, the mono- and bisanthrapyrazoles with methyl amino groups in the side chain or the linker, respectively, was nearly parallel to that of the other plot (both −0.14 log units/°). These results suggests that the strength of DNA binding was, in part, responsible for the growth inhibitory activity of these compounds. We previously found that the ΔT_m values were well correlated with K562 $\log IC_{50}$ values for a series of monoanthrapyrazoles with amino side chains[3] and with netropsin-like oligopyrrole side chains,[6] though there was no correlation found for a series of ester- and amide-linked bisanthrapyrazoles.[4,5]

3. Discussion

A series of monoanthrapyrazoles with piperazine side chains and bisanthrapyrazole derivatives containing piperazine linkers were synthesized and compared for their ability to inhibit K562 and K/VP.5 cell growth. Most of the compounds (**16**, **17**, **18**, **21**, and **24**) achieved submicromolar IC_{50} values. The bisanthrapyrazoles with longer linkers (**16**, **17**, **18**, and **21**) were the most potent in inhibiting cell growth (Table 1). Compound **18** with a six-carbon linker was the most potent compound tested. Depending upon the particular compound, the piperazine amino groups and/or the methyl amino groups would be partially mono- or diprotonated at physiological pH which would contribute to DNA binding through electrostatic interactions. It was calculated (ChemAxon, http://www.chemaxon.com) that for compounds **15** and **24** the major microspecies would be monoprotonated, whereas for all of the other compounds (**16**, **17**, **18**, **21**, and **23**) the major microspecies

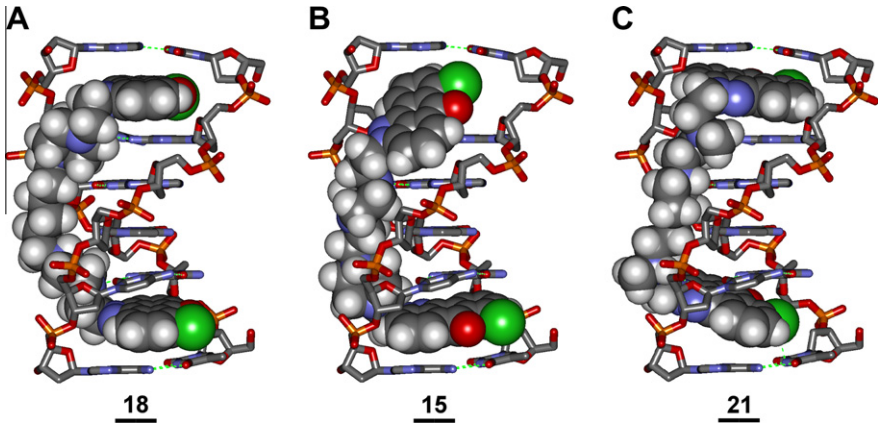

Figure 5. Docking of bisanthrapyrazoles into an X-ray structure of DNA. (A) The highest scoring structure of diprotonated **18** with a six-methylene linker docked into the 1DA9 X-ray structure of a DNA-(doxorubicin)$_2$ complex.[34] (B) The highest scoring structure of monoprotonated **15** with a two-methylene linker docked into the same X-ray structure. (C) The highest scoring structure of diprotonated **21** with a two methyl amino groups in the linker docked into the same X-ray structure. The H-atoms of the DNA are not shown for clarity. The doxorubicin-bound ligands were removed and the compounds were docked into their place with the genetic algorithm docking program GOLD. While compound **18** displayed good bisintercalation, compound **15** achieved only monointercalation with the other anthrapyrazole group in the minor groove. Compound **21** also achieved bisintercalation though not as good as compound **18** with its longer linker.

would be diprotonated and hence dicationic. For example, for compound **16** the two equivalent major diprotonated species at pH 7.4 are 46% of all species. For these two species the piperazine nitrogen closest to the anthrapyrazole is protonated, and the piperazine nitrogen furthest away from the other anthrapyrazole is as well. The two equivalent monoprotonated species for compound **16** are on the piperazine nitrogen furthest away from the anthrapyrazole for a total of 34% of all species. The fact that the dications **16**, **17**, **18**, and **21** displayed submicromolar potency suggest that the dications were readily able to enter the cells to exert their growth inhibitory effects.

All of the compounds tested (Table 1) strongly inhibited the decatenation activity of topoisomerase IIα (Fig. 3A). However, these compounds, at least compared to the etoposide positive control, produced little or no measurable linear DNA and thus were not potent topoisomerase IIα poisons (Fig. 3B). It should also be noted that doxorubicin, which is generally acknowledged to target topoisomerase II and act as a poison,[36] did not, as we previously showed,[6] cause DNA cleavage indicative of topoisomerase IIα-DNA covalent complex formation (Table 1). Thus, if these compounds were growth inhibitory by acting on topoisomerase IIα, they likely exerted their action primarily by inhibiting topoisomerase II catalytic activity, and not by stabilizing the DNA-topoisomerase IIα cleavage complex. The lack of cross resistance to the K/VP.5 cell line with reduced topoisomerase IIα levels also supports the conclusion that these compounds did not act as topoisomerase II poisons. This result is in contrast to several of the mono- and bisanthrapyrazoles and anthrapyrazole-netropsin combilexins we previously studied which do act as topoisomerase IIα poisons.[3–6] Compounds that bind strongly to DNA generally inhibit the catalytic activity of topoisomerase II, probably by interfering with formation of the topoisomerase II-DNA complex.

Compounds **23** and **24**, both monoanthrapyrazoles, strongly inhibited the relaxation activity (Table 1) of topoisomerase I (Fig. 4). Again, it is likely that the inhibition of the topoisomerase I catalytic activity was due to these two compounds binding to DNA and interfering with the relaxation reaction. Thus, both the mono- and bisanthrapyrazoles may be inhibiting cell growth through their ability to inhibit both topoisomerase I and topoisomerase II.

The results of docking the compounds into the X-ray structures of a doxorubicin-DNA (Fig. 5A–C) complex showed that compound **15** with a two-carbon linker could only act as a monointercalator. Compound **15**, however, docked well into the minor groove of an X-ray structure of the netropsin-DNA complex. It was not possible, therefore, to distinguish between these two possible binding modes based on the docking studies. Thus, compound **15** may be a minor groove binder, or possibly even a mixed minor groove binder-monointercalator. However, compound **16** appeared to achieve at least partial bisintercalation, whereas compounds **17**, **18**, and **21** with longer linkers could readily dock into the DNA and achieve bisintercalation. These conclusions are also supported by the results of Figure 2 in which the concentration dependence of ΔT_m was compared for the mono- and bisanthrapyrazoles, and in which it was shown that the bisintercalators with sufficiently long linkers had slopes that were approximately two-fold or greater than their corresponding monoanthrapyrazoles. There is no physical proof that **23** and **24** are monointercalators rather than groove binders as it is possible that the changes in ΔT_m could be due to groove binding. The best argument in favor of monointercalation is that **23** and **24** are planar aromatic tri-cyclic compounds structurally similar to doxorubicin which has been shown by X-ray to be an intercalator (www.rcsb.org/pdb/; PDB ID: 1DA9).[34] The second argument is that these compounds preferentially docked into the doxorubicin binding site rather than in the DNA groove.

LogIC_{50} values for K562 cell growth inhibition for both mono- and bisintercalators were reasonably well correlated with ΔT_m (Fig. 6), indicating that the strength of DNA binding was a reasonable predictor of cell growth inhibition. However, the strength of DNA binding was probably not the only factor that determined cell growth inhibitory activity. All of the mono- and bisanthrapyrazoles strongly inhibited the catalytic activity of topoisomerase IIα (Fig. 3). Because all these compounds bound to DNA to varying degrees, it was not surprising that they interfered with the catalytic activity of both topoisomerase I and topoisomerase II which utilize DNA as their substrate. The mono- and bisanthrapyrazoles, by virtue of their ability to bind to DNA, may also have inhibited other DNA processing enzymes which could also contribute to inhibition of cell growth. Biological and physical evaluation data for the most growth inhibitory ester- or amide-linked bisanthrapyrazoles (**25** and **26**, respectively) previously synthesized,[4,5] are compared in Table 1. The most potent piperazine-linked bisanthrapyrazole **18** was about 5–20-fold more growth inhibitory towards K562 cells than our ester- or amide-linked bisanthrapyrazoles **25** and **26**, respectively.[4,5] Compound **18** achieved an IC_{50} value equal to that for lososoxantrone.[4] Compound **18** was also about as potent towards

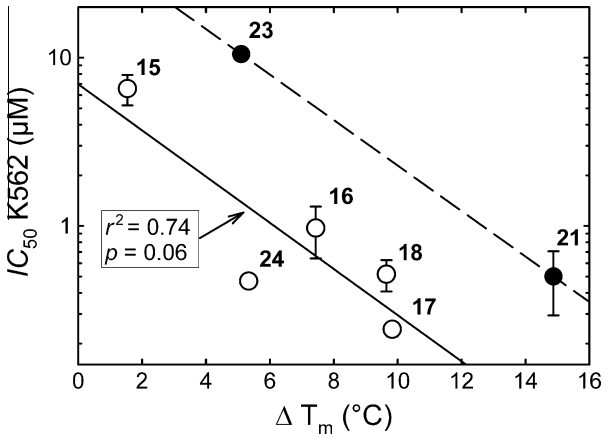

Figure 6. QSAR correlations of strength of DNA binding as measured by ΔT_m with the logarithm of IC_{50} for K562 cell growth inhibition by two series of piperazine-linked mono- and bisanthrapyrazoles. The solid line is the least-squares calculated best fit for the correlation for the mono- and bisanthrapyrazoles **15**, **16**, **17**, **18**, and **24** (open circles). The broken line connecting the data for the compounds **23** and **21**, the mono- and bisanthrapyrazoles with methyl amino groups in the side chain or the linker respectively (closed circles), is close to parallel to that for the mono- and bispiperazine-linked compounds. The errors bars are SEMs and where not shown are smaller than the size of the symbol.

K562 cells as some of our most potent anthrapyrazole-netropsin combilexins.[6] Also, neither **25** nor **26** increased ΔT_m as much as compound **18**, nor did they inhibit topoisomerase IIα decatenation activity as much.

In summary, a series of monoanthrapyrazoles with piperazine side chains and bisanthrapyrazole compounds containing piperazine linkers were synthesized and tested for their ability to inhibit cancer cell growth. The bisanthrapyrazoles were designed to both bisintercalate and bind in the DNA minor groove through interaction with the positively charged piperazine linkers. As predicted from the docking results, the bisanthrapyrazoles that achieved bisintercalation were those that had three or more carbon linkers enabling them to span four DNA base pairs. The compounds also bound DNA the strongest and had the greatest cell growth inhibitory activity. The compounds that were predicted to be dications through protonation of the amino groups in the linkers or side chains were also much more potent in inhibiting cell growth than the mono cationic compounds.

Finally, it is of some interest that an X-ray structure of etoposide bound to the covalent DNA-topoisomerase IIβ cleavable complex has just been published.[37] Etoposide is a weak DNA intercalator (dissociation constant 11 μM).[38,39] However, in this newly published structure two molecules of etoposide separated by four intervening base pairs, are intercalated into the cleaved duplex DNA in which the base pairs directly next to the etoposide molecules bulge out to accommodate the bound etoposide molecules. Bisintercalators similar to compounds **17** and **18** that are capable of spanning four DNA base pairs could, in principle, similarly bind to a covalent DNA-topoisomerase II cleavable complex. Hence, our forward development of bisintercalators similar to those synthesized in this study may lead to more efficacious topoisomerase II inhibitors.

4. Experimental

4.1. Biological assays

4.1.1. Materials, cell culture, growth inhibition assays

The plasmid DNA and the absorbance-based cell proliferation assay and other materials were as previously described.[4–6] Human leukemia K562 cells, obtained from the American Type Culture Collection and K/VP.5 cells (a 26-fold etoposide-resistant K562-derived sub-line with decreased levels of topoisomerase IIα mRNA and protein)[30] were maintained as suspension cultures in αMEM (Minimal Essential Medium Alpha, Invitrogen, Burlington, Canada) containing 10% fetal calf serum. The spectrophotometric 96-well plate cell growth inhibition 3-(4,5-dimethylthiazol-2-yl)-5-(3-carboxymethoxyphenyl)-2-(4-sulfophenyl)-2H-tetrazolium (MTS) CellTiter 96 AQueous One Solution Cell Proliferation assay, which measures the ability of the cells to enzymatically reduce MTS after drug treatment, has been described.[3,6] The drugs were dissolved in DMSO and the final concentration of DMSO did not exceed an amount that had any detectable effect on cell growth. The cells were incubated with the drugs for 72 h and then assayed with MTS. The IC_{50} values for cell growth inhibition were measured by fitting the absorbance-drug concentration data to a four-parameter logistic equation as described.[4–6] The errors quoted are standard error of the means (SEMs) and typically gave% SEMs of about 20%.

4.1.2. Topoisomerase IIα kDNA decatenation, pBR322 DNA relaxation, and cleavage assays

A gel assay as previously described[6,23] was used to determine if the compounds of Table 1 inhibited the catalytic decatenation activity of topoisomerase IIα. kDNA, which consists of highly catenated networks of circular DNA, is decatenated by topoisomerase IIα in an ATP-dependent reaction to yield individual minicircles of DNA. The assay conditions and the expression, extraction, and purification of recombinant full-length human topoisomerase IIα were previously described.[4–6,40] The percentage decatenation was obtained through densitometric analysis of the bands relative to that obtained for the fully decatenated closed circular DNA alone (arbitrarily set to 100% for the control in the absence of drug). The percentage inhibition was calculated from 100 minus the percentage relative integrated band intensity.

Topoisomerase II-cleaved DNA complexes produced by anticancer drugs may be trapped by rapidly denaturing the complexed enzyme with sodium dodecyl sulfate (SDS).[26] The drug-induced cleavage of double-stranded closed circular pBR322 DNA to form linear DNA at 37 °C was followed by separating the SDS-treated reaction products using ethidium bromide gel electrophoresis essentially as described, except that all components of the assay mixture were assembled and mixed on ice prior to addition of the drug.[4–6,26] The percentage cleavage was obtained through densitometric analysis of the linear DNA bands relative to that obtained for linear DNA produced by 50 μM etoposide (arbitrarily set to 100%) less the amount produced by the no-drug control.

4.1.3. Topoisomerase I inhibition of pBR322 DNA relaxation assay

A gel assay as previously described[28] was used to determine if the compounds of Table 1 inhibited topoisomerase I. The pBR322 DNA was from MBI Fermentas (Burlington, Canada). Cellular nuclear extract, prepared as described,[41] was used as the source of topoisomerase I. The 20 μL assay mixture contained 60 ng of pBR322 DNA, 50 ng of nuclear extract protein and 20 μM of the test drugs. After a 20 min incubation at 37 °C in assay buffer the reaction was terminated with 0.05% (v/v) SDS. Electrophoresis was carried out as for the topoisomerase IIα cleavage assay, except that neither the gel nor the running buffer contained ethidium bromide in order to obtain good separation of the relaxed and supercoiled DNA. In the absence of ethidium bromide the supercoiled DNA runs ahead of the relaxed DNA. The percentage inhibition was obtained through densitometric analysis of the supercoiled bands relative to that obtained for pBR322 DNA alone (arbitrarily set to 100%) in the absence of enzyme.

4.1.4. Thermal denaturation of DNA assay

Compounds that either intercalate into or bind in the minor groove of DNA stabilize the DNA double helix and increase the temperature at which the DNA denatures or unwinds.[20,42,43] The effect of 0, 0.1, 0.2, 0.4, 1.0, and 2 μM of the compounds on the increase in DNA melting temperature, ΔT_m, of sonicated calf thymus DNA (5 μg/mL or 7.7 μM in base pairs) was measured in 10 mM Tris–HCl buffer (pH 7.4) in a Cary 1 (Varian, Mississauga, Canada) double beam spectrophotometer by measuring the absorbance increase at 260 nm upon the application of a temperature ramp of 1 °C/min as we previously described.[3–6] Doxorubicin, which is a strong DNA intercalator, was used as a positive control.[3–6] A plot of the drug concentration versus ΔT_m was used to obtain linear least-squares calculated fits to the equation ΔT_m = slope·[anthrapyrazole]. Because T_m was determined multiple times and was known much more accurately, the intercepts in the plots were forced through the origin. The best-fit calculated slopes were used to calculate ΔT_m values at a drug concentration of 1 μM. The SEMs of the slopes were typically about 1 °C/μM. The experiments were designed using relatively low anthrapyrazole concentrations to yield linear plots.

4.2. Molecular modeling and docking

4.2.1. Docking of the mono- and bisanthrapyrazole piperazines into an X-ray structure of DNA and calculation of protonated microspecies

The molecular modeling and the docking were carried out as previously described.[4,6] The major protonated microspecies present at pH 7.4 were docked either into the doxorubicin binding site of a six-base pair X-ray crystal structure of two molecules of doxorubicin bound to double stranded DNA, d(TGGCCA)/doxorubicin, (www.rcsb.org/pdb/; PDB ID: 1DA9)[34] or in the case of **15** into a 12-base pair X-ray structure of a molecule of netropsin (PDB ID: 195D)[35] bound to the minor groove of double stranded DNA, d(CGCGTTAACGCG)/netropsin, using the genetic algorithm docking program GOLD version 3.2[44] with default GOLD parameters and atom types and with 500 starting runs as previously described.[4–6] The two doxorubicin molecules in the 1DA9 DNA X-ray structure are separated by four intervening base pairs. The first and second base pairs buckle out to accommodate the bound doxorubicin in this structure.[34] The DNA structures were prepared by removing the doxorubicin or netropsin molecules and the water molecules to avoid potential interference with the docking. Ligand structures were energy minimized before docking and local optimization of the ligand conformation was done at the end of the run. Hydrogens were added to the DNA with the SYBYL Biopolymer module.[45] The binding site (6 Å radius) was defined using a previously docked amide-linked bisanthrapyrazole that docked both intercalated and in the minor groove[5] for the 1DA9 structure or netropsin in the 195D structure. Doxorubicin and netropsin docked back into their respective DNA structures with a heavy atom root-mean-squared distance of 1.3 and 0.32 Å, respectively, compared to their X-ray structures.[34,35] Values of 2.0 Å or less in the extensive GOLD test set are considered to be good.[46] The graphic was prepared with DS Visualizer 2.5 (Accelrys, San Diego, CA). MarvinSketch and its associated calculator plugins were used for displaying the mono- and bisanthrapyrazoles and calculating their pK_a values and the major protonated microspecies present at pH 7.4 (Marvin version 5.3.6, 2010, ChemAxon, http://www.chemaxon.com).

4.3. Chemistry

4.3.1. General

^{1}H and ^{13}C nuclear magnetic resonance (NMR) spectra were recorded at 300 K in 5 mm NMR tubes on a Bruker Avance 300 MHz NMR spectrometer operating at 300.13 MHz for ^{1}H NMR and 75.5 MHz for ^{13}C NMR, respectively, in $CDCl_3$. Chemical shifts are given in parts per million (ppm) (±0.01 ppm) relative to tetramethylsilane (0.00 ppm) in the case of the ^{1}H NMR spectra, and to the central line of $CDCl_3$ (δ 77.0) for the ^{13}C NMR spectra. Melting points were taken on a Gallenkamp (Loughborough, England) melting point apparatus and were uncorrected. The high resolution mass spectra were run on an Agilent 6210 Accurate-Mass Time-of-Flight (TOF) LC/MS system (Agilent Technologies, Mississauga, Canada) using electrospray ionization. The samples were dissolved in methanol and were infused into the mass spectrometer with an Agilent 1200 HPLC using acetonitrile/water containing 0.1% (v/v) formic acid as the mobile phase. TLC was performed on plastic-backed plates bearing 200 μm silica gel 60 F_{254} (Silicycle, Quebec City, Canada). Compounds were visualized by quenching of fluorescence by UV light (254 nm) where applicable. The reaction conditions were not optimized for reaction yields. All chemicals were from Aldrich (Oakville, Canada) and were used as received. 7-Chloro-2-(2-methanesulfonyloxyethyl)anthra[1,9-*cd*]pyrazol-6(2*H*)-one **14** and 7-chloro-2-[2-[(2-chloroethyl)methylamino]ethyl]anthra[1,9-*cd*]pyrazol-6(2*H*)-one **19** were prepared as we previously described.[5,6] The procedures for making the *t*-Boc-protected bispiperazines **6**–**9** and their deprotection to obtain the bispiperazines **10**–**13** were as described.[18] The synthesis of compounds **6** and **10** were prepared as described.[18] Compounds **7**, **9**, **11**, and **13** have been previously reported,[47] and were also made as described.[18] The structures of compounds **6**, **7**, **9**, **10**, **11**, and **13** were confirmed by ^{1}H NMR and MS (ESI).

4.3.2. 1,4-Bis(4-((*tert*-butoxyl)carbonyl)piperazin-1-yl)-2-trans-butene (8)

Compound **8** was prepared using the procedures described.[18] *tert*-Butyl piperazine-1-carboxylate **1**, (*E*)-1,4-dibromobut-2-ene **4** and potassium carbonate in ethanol were refluxed overnight. After working up as described[18] and recrystallization in ethanol/water (1:1 v/v), compound **8** was obtained as needle-shaped white crystals in 80% yield; mp: 115–116 °C; ^{1}H NMR ($CDCl_3$) δ 5.64 (m, 2H), 3.41 (t, J = 4.9 Hz, 8H), 2.96–2.98 (m, 4H), 2.35 (t, J = 4.9 Hz, 8H), 1.44 (s, 18H); ^{13}C NMR ($CDCl_3$) δ 154.75, 130.31, 79.64, 60.53, 52.89, 28.44; HRMS (ESI), m/z (M+H)$^+$: calcd 425.3122, obsd 425.3126.

4.3.3. 1,4-Bis(piperazin-1-yl)-2-*trans*-butene (12)

Compound **8** was treated with trifluoroacetic acid/dichloromethane (1:3 v/v)[18] to give compound **12** as a white solid in 98% yield; mp: 107–108 °C; ^{1}H NMR ($CDCl_3$) δ 5.67 (m, 2H), 2.98 (m, 4H), 2.90 (t, J = 4.8 Hz, 8H), 2.41 (br, 8H); ^{13}C NMR ($CDCl_3$) δ 130.30, 61.18, 54.45, 46.07; HRMS (ESI), m/z (M+H)$^+$: calcd 225.2074, obsd 225.2076.

4.3.4. General procedure for the syntheses of the anthrapyrazole-piperazine compounds

The anthrapyrazoles **14** and **19** were reacted with the corresponding piperazines or bispiperazines in acetonitrile in the presence of K_2CO_3 at 60 °C overnight. The mixtures were then cooled to room temperature, filtered and the solvent was removed under vacuum. The desired products were purified by column chromatography (silica gel) using dichloromethane/methanol/triethylamine (10:1:2 v/v/v) as an eluant.

4.3.5. 1,2-Bis(*N*-(2-(7-chloro-6-oxo-6*H*-dibenzo[*cd*,*g*]indazol-2-yl)-ethyl)-piperazin-1-yl)ethane (15)

The bispiperazine **10** was reacted with **14** in a 1:2.2 molar ratio to produce **15** as a reddish-orange solid in 42% yield; mp: 106–107 °C; ^{1}H NMR ($CDCl_3$) δ 8.20 (dd, J_1 = 6.5 Hz, J_2 = 2.5 Hz, 2H), 8.00 (d, J = 6.9 Hz, 2H), 7.61–7.72 (m, 4H), 7.51–7.58 (m, 4H),

4.62 (t, J = 6.7 Hz, 4H), 2.95 (t, J = 6.7 Hz, 4H), 2.47–2.56 (m, 20H); ^{13}C NMR ($CDCl_3$) δ 182.74, 139.33, 138.29, 137.25, 134.76, 132.93, 132.66, 129.16, 128.50, 127.01, 122.80, 121.79, 120.97, 114.95, 57.82, 55.85, 53.61, 53.41, 48.23; HRMS (ESI), m/z $(M+H)^+$: calcd 759.2724, obsd 759.2751.

4.3.6. 1,3-Bis(*N*-(2-(7-chloro-6-oxo-6*H*-dibenzo[*cd*,*g*]indazol-2-yl)-ethyl)-piperazin-1-yl)propane (16)

The bispiperazine **11** was reacted with **14** in a 1:2.2 mole ratio to produce **16** as a reddish-orange solid in 45% yield; mp: 98–100 °C; ^{1}H NMR ($CDCl_3$) δ 8.19 (dd, J_1 = 6.5 Hz, J_2 = 2.5 Hz, 2H), 7.99 (d, J = 6.6 Hz, 2H), 7.60–7.71 (m, 4H), 7.51–7.58 (m, 4H), 4.62 (t, J = 6.7 Hz, 4H), 2.96 (t, J = 6.7 Hz, 4H), 2.57 (br, 8H), 2.42 (br, 8H), 2.32 (t, J = 6.7 Hz, 4H) 1.66 (m, 2H); ^{13}C NMR ($CDCl_3$) δ 182.69, 139.29, 138.22, 137.21, 134.74, 132.90, 132.52, 129.12, 128.47, 126.95, 122.76, 121.78, 120.93, 114.95, 57.82, 55.85, 53.61, 53.41, 48.23; HRMS (ESI), m/z $(M+H)^+$: calcd 773.2881, obsd 773.2890.

4.3.7. 1,4-Bis(*N*-(2-(7-chloro-6-oxo-6*H*-dibenzo[*cd*,*g*]indazol-2-yl)-ethyl)-piperazin-1-yl)-2-trans-butene (17)

The bispiperazine **12** was reacted with **14** in a 1:2.2 mole ratio to produce **17** as a reddish-orange solid in 40% yield; mp: 110–111 °C; ^{1}H NMR ($CDCl_3$) δ 8.20–8.23 (m, 2H), 8.01 (d, J = 6.9 Hz, 2H), 7.74–7.53 (m, 8H), 5.63–5.69 (m, 2H), 4.65 (dt, J_1 = 6.6 Hz, J_2 = 1.9 Hz, 4H), 2.95–3.03 (m, 8H), 2.54–2.62 (m, 8H), 2.40–2.48 (m, 8H); ^{13}C NMR ($CDCl_3$) δ 182.74, 139.35, 138.30, 137.26, 134.77, 132.94, 132.57, 129.18, 128.55, 128.52, 127.02, 122.81, 121.80, 120.98, 114.97, 60.40, 60.35, 57.82, 53.38, 53.04, 48.24, 48.22, 45.84; MS (ESI m/z): HRMS (ESI), m/z $(M+H)^+$: calcd 785.2881, obsd 785.2910.

4.3.8. 1,6-Bis(*N*-(2-(7-chloro-6-oxo-6*H*-dibenzo[*cd*,*g*]indazol-2-yl)-ethyl)-piperazin-1-yl)hexane (18)

The bispiperazine **13** was reacted with **14** in a 1:2.2 mole ratio to produce **18** as a reddish-orange solid in 50% yield; mp: 93–94 °C; ^{1}H NMR ($CDCl_3$) δ 8.19 (dd, J_1 = 6.4 Hz, J_2 = 2.5 Hz, 2H), 7.98 (d, J = 6.9 Hz, 2H), 7.60–7.71 (m, 4H), 7.50–7.57 (m, 4H), 4.62 (t, J = 6.8 Hz, 4H), 2.96 (t, J = 6.8 Hz, 4H), 2.58 (br, 8H), 2.27–2.45 (m, 12H), 1.39–1.54 (m, 4H) 1.24–1.36 (m, 4H); ^{13}C NMR ($CDCl_3$) δ 182.67, 139.30, 138.21, 137.20, 134.75, 132.90, 132.51, 129.12, 128.47, 126.95, 122.76, 121.79, 120.92, 114.98, 58.64, 57.85, 53.43, 53.21, 48.21, 27.51, 26.80; HRMS (ESI), m/z $(M+H)^+$: calcd 815.3350, obsd 815.3355.

4.3.9. *N*,*N*-Bis(2-((2-(7-chloro-6-oxo-6*H*-dibenzo[*cd*,*g*]indazol-2-yl)ethyl)-methylamino)ethyl) piperazine (21)

The piperazine **20** was reacted with **19** in a 1:2.2 mole ratio to produce **21** as a reddish-orange solid in 38% yield; mp: 90–92 °C; ^{1}H NMR ($CDCl_3$) δ 8.18 (dd, J_1 = 5.6 Hz, J_2 = 2.3 Hz, 1H), 7.96 (d, J = 7.0 Hz, 1H), 7.50–7.70 (m, 4H), 4.58 (t, J = 6.6 Hz, 2H), 3.00 (t, J = 6.6 Hz, 2H), 2.56 (t, J = 6.9 Hz, 2H), 2.34–2.39 (m, 13H), 2.23 (s, 3H); ^{13}C NMR ($CDCl_3$) δ 182.68, 139.40, 138.13, 137.20, 134.78, 132.92, 132.50, 129.10, 128.53, 126.93, 122.72, 121.77, 120.91, 115.08, 57.49, 56.05, 55.18, 53.04, 48.60, 42.79; HRMS (ESI), m/z $(M+H)^+$: calcd 761.2881, obsd 761.2879.

4.3.10. 7-Chloro-2-[2-[(2-(4-methyl-piperazin-1-yl)ethyl)methylamino]ethyl]-anthra[1,9-*cd*]pyrazol-6(2*H*)-one (23)

1-Methylpiperazine **22** was reacted with **19** in a 1:1.1 mole ratio to produce **23** as a reddish-orange solid in 57% yield; mp: 113–115 °C; ^{1}H NMR ($CDCl_3$) δ 8.16 (dd, J_1 = 5.6 Hz, J_2 = 2.3 Hz, 1H), 7.96 (d, J = 7.0 Hz, 1H), 7.50–7.70 (m, 4H), 4.58 (t, J = 6.6 Hz, 2H), 3.00 (t, J = 6.6 Hz, 2H), 2.56 (t, J = 6.9 Hz, 2H), 2.34–2.39 (m, 13H), 2.23 (s, 3H); ^{13}C NMR ($CDCl_3$) δ 182.67, 139.32, 138.14, 137.18, 134.75, 132.90, 132.48, 129.09, 128.50, 126.92, 122.72, 121.76, 120.91, 114.96, 57.51, 56.27, 55.27, 54.86, 53.38, 48.65, 45.88, 42.91; HRMS (ESI), m/z $(M+H)^+$: calcd 438.2055, obsd 438.2070.

4.3.11. 7-Chloro-2-(2-(piperazin-1-yl)ethyl)anthra[1,9-*cd*]pyrazol-6(2*H*)-one (24)

Piperazine **20** was reacted with 14 in a 1.5:1 mole ratio to produce **24** as a reddish-orange solid in 50% yield; mp: 121–122 °C; ^{1}H NMR ($CDCl_3$) δ 8.18 (dd, J_1 = 6.6 Hz, J_2 = 2.5 Hz, 1H), 7.97 (d, J = 6.6 Hz, 1H), 7.49–7.71 (m, 4H), 4.62 (t, J = 6.7 Hz, 2H), 2.94 (t, J = 6.7 Hz, 2H), 2.84 (t, J = 4.7 Hz, 4H), 2.50 (t, J = 4.7 Hz, 4H); ^{13}C NMR ($CDCl_3$) δ 182.70, 139.32, 138.22, 137.20, 134.76, 132.90, 132.50, 129.13, 128.47, 126.95, 122.76, 121.77, 120.93, 114.97, 58.48, 54.75, 48.10, 46.09; HRMS (ESI), m/z $(M+H)^+$: calcd 367.1320, obsd 367.1388.

Acknowledgments

Supported by grants from the Canadian Institutes of Health Research, the Canada Research Chairs Program, a Canada Research Chair in Drug Development to Brian Hasinoff and an NIH Grant CA090787 to Jack Yalowich.

Supplementary data

Supplementary data associated with this article can be found, in the online version, at doi:10.1016/j.bmc.2011.10.012. These data include MOL files and InChiKeys of the most important compounds described in this article.

References and notes

1. Nitiss, J. L. *Nat. Rev. Cancer* **2009**, *9*, 327.
2. Nitiss, J. L. *Nat. Rev. Cancer* **2009**, *9*, 338.
3. Liang, H.; Wu, X.; Guziec, L. J.; Guziec, F. S., Jr.; Larson, K. K.; Lang, J.; Yalowich, J. C.; Hasinoff, B. B. *J. Chem. Inf. Model.* **2006**, *46*, 1827.
4. Hasinoff, B. B.; Liang, H.; Wu, X.; Guziec, L. J.; Guziec, F. S., Jr.; Yalowich, J. C. *Bioorg. Med. Chem.* **2008**, *16*, 3959.
5. Hasinoff, B. B.; Zhang, R.; Wu, X.; Guziec, L. J.; Guziec, F. S., Jr.; Marshall, K.; Yalowich, J. C. *Bioorg. Med. Chem.* **2009**, *17*, 4575.
6. Zhang, R.; Wu, X.; Guziec, L. J.; Guziec, F., Jr.; Chee, G.-L.; Yalowich, J. C.; Hasinoff, B. B. *Bioorg. Med. Chem.* **2010**, *18*, 3974.
7. Antonini, I.; Santoni, G.; Lucciarini, R.; Amantini, C.; Sparapani, S.; Magnano, A. *J. Med. Chem.* **2006**, *49*, 7198.
8. Gago, F. *Methods* **1998**, *14*, 277.
9. Pindur, U.; Jansen, M.; Lemster, T. *Curr. Med. Chem.* **2005**, *12*, 2805.
10. Martinez, R.; Chacon-Garcia, L. *Curr. Med. Chem.* **2005**, *12*, 127.
11. Zolova, O. E.; Mady, A. S.; Garneau-Tsodikova, S. *Biopolymers* **2010**, *93*, 777.
12. Dawson, S.; Malkinson, J. P.; Paumier, D.; Searcey, M. *Nat. Prod. Rep.* **2007**, *24*, 109.
13. Cholody, W. M.; Kosakowska-Cholody, T.; Hollingshead, M. G.; Hariprakasha, H. K.; Michejda, C. J. *J. Med. Chem.* **2005**, *48*, 4474.
14. Galisteo, J.; Navarro, P.; Campayo, L.; Yunta, M. J.; Gomez-Contreras, F.; Villa-Pulgarin, J. A.; Sierra, B. G.; Mollinedo, F.; Gonzalez, J.; Garcia-Espana, E. *Bioorg. Med. Chem.* **2010**, *18*, 5301.
15. Szumilak, M.; Szulawska-Mroczek, A.; Koprowska, K.; Stasiak, M.; Lewgowd, W.; Stanczak, A.; Czyz, M. *Eur. J. Med. Chem.* **2010**, *45*, 5744.
16. Casero, R. A., Jr.; Woster, P. M. *J. Med. Chem.* **2009**, *52*, 4551.
17. Gentry, A. C.; Pitts, S. L.; Jablonsky, M. J.; Bailly, C.; Graves, D. E.; Osheroff, N. *Biochemistry* **2011**, *50*, 3240.
18. Edwards, C.; Ray, N. C.; Gill, M. I. A.; Alcindor, J.; Finch, H.; Fitzgerald, M. F. WO 2007042815, **2007**.
19. Bjorndal, M. T.; Fygenson, D. K. *Biopolymers* **2002**, *65*, 40.
20. McGhee, J. D. *Biopolymers* **1976**, *15*, 1345.
21. Fortune, J. M.; Osheroff, N. *Prog. Nucleic Acid Res. Mol. Biol.* **2000**, *64*, 221.
22. Li, T. K.; Liu, L. F. *Annu. Rev. Pharmacol. Toxicol.* **2001**, *41*, 53.
23. Hasinoff, B. B.; Kozlowska, H.; Creighton, A. M.; Allan, W. P.; Thampatty, P.; Yalowich, J. C. *Mol. Pharmacol.* **1997**, *52*, 839.
24. Leteurtre, F.; Kohlhagen, G.; Paul, K. D.; Pommier, Y. *J. Natl. Cancer Inst.* **1994**, *86*, 1239.
25. Capranico, G.; Palumbo, M.; Tinelli, S.; Mabilia, M.; Pozzan, A.; Zunino, F. *J. Mol. Biol.* **1994**, *28*, 1218.
26. Burden, D. A.; Froelich-Ammon, S. J.; Osheroff, N. *Methods Mol. Biol.* **2001**, *95*, 283.
27. Hasinoff, B. B.; Wu, X.; Begleiter, A.; Guziec, L.; Guziec, F. S., Jr.; Giorgianni, A.; Yang, S.; Jiang, Y.; Yalowich, J. C. *Cancer Chemother. Pharmacol.* **2006**, *57*, 221.

28. Liang, H.; Wu, X.; Yalowich, J. C.; Hasinoff, B. B. *Mol. Pharmacol.* **2008**, *73*, 686.
29. Pommier, Y.; Pourquier, P.; Fan, Y.; Strumberg, D. *Biochim. Biophys. Acta* **1998**, *1400*, 83.
30. Fattman, C.; Allan, W. P.; Hasinoff, B. B.; Yalowich, J. C. *Biochem. Pharmacol.* **1996**, *52*, 635.
31. Ritke, M. K.; Allan, W. P.; Fattman, C.; Gunduz, N. N.; Yalowich, J. C. *Mol. Pharmacol.* **1994**, *46*, 58.
32. Ritke, M. K.; Roberts, D.; Allan, W. P.; Raymond, J.; Bergoltz, V. V.; Yalowich, J. C. *Br. J. Cancer* **1994**, *69*, 687.
33. Ritke, M. K.; Rusnak, J. M.; Lazo, J. S.; Allan, W. P.; Dive, C.; Heer, S.; Yalowich, J. C. *Mol. Pharmacol.* **1994**, *46*, 605.
34. Leonard, G. A.; Hambley, T. W.; McAuley-Hecht, K.; Brown, T.; Hunter, W. N. *Acta Crystallogr. D. Biol. Crystallogr.* **1993**, *49*, 458.
35. Balendiran, K.; Rao, S. T.; Sekharudu, C. Y.; Zon, G.; Sundaralingam, M. *Acta Crystallogr. D. Biol. Crystallogr.* **1995**, *51*, 190.
36. Gewirtz, D. A. *Biochem. Pharmacol.* **1999**, *57*, 727.
37. Wu, C. C.; Li, T. K.; Farh, L.; Lin, L. Y.; Lin, T. S.; Yu, Y. J.; Yen, T. J.; Chiang, C. W.; Chan, N. L. *Science* **2011**, *333*, 459.
38. Chow, K. C.; Macdonald, T. L.; Ross, W. E. *Mol. Pharmacol.* **1988**, *34*, 467.
39. Ross, W.; Rowe, T.; Glisson, B.; Yalowich, J.; Liu, L. *Cancer Res.* **1984**, *44*, 5857.
40. Hasinoff, B. B.; Wu, X.; Krokhin, O. V.; Ens, W.; Standing, K. G.; Nitiss, J. L.; Sivaram, T.; Giorgianni, A.; Yang, S.; Jiang, Y.; Yalowich, J. C. *Mol. Pharmacol.* **2005**, *67*, 937.
41. Hasinoff, B. B.; Kuschak, T. I.; Creighton, A. M.; Fattman, C. L.; Allan, W. P.; Thampatty, P.; Yalowich, J. C. *Biochem. Pharmacol.* **1997**, *53*, 1843.
42. Sissi, C.; Leo, E.; Moro, S.; Capranico, G.; Mancia, A.; Menta, E.; Krapcho, A. P.; Palumbo, M. *Biochem. Pharmacol.* **2004**, *67*, 631.
43. Priebe, W.; Fokt, I.; Przewloka, T.; Chaires, J. B.; Portugal, J.; Trent, J. O. *Methods Enzymol.* **2001**, *340*, 529.
44. GOLD 3.2, CCDC Software Ltd, Cambridge, UK.
45. SYBYL 7.3, Tripos Inc., 1699 South Hanley Rd., St. Louis, MO, 63144, USA.
46. Verdonk, M. L.; Cole, J. C.; Hartshorn, M. J.; Murray, C. W.; Taylor, R. D. *Proteins* **2003**, *52*, 609.
47. Li, R.; Cheng, T.; Li, C.; Gao, F.; Wang, X.; Zhang, H. CN1344717A, **2002**.